Truncated Form of the Epstein-Barr Virus Protein EBNA-LP Protects against Caspase-Dependent Apoptosis by Inhibiting Protein Phosphatase 2A[∇]

Julie Garibal,[1] Émilie Hollville,[1] Andrew I. Bell,[2] Gemma L. Kelly,[2] Benjamin Renouf,[1]
Yasushi Kawaguchi,[3] Alan B. Rickinson,[2] and Joëlle Wiels[1]*

*UMR 8126 CNRS, University Paris-Sud, Institut Gustave Roussy, 94805 Villejuif cedex, France[1]; Cancer Research UK Institute for
Cancer Studies, University of Birmingham, Edgbaston, Birmingham, B15 2TT, United Kingdom[2]; and Department of
Infectious Disease Control, The Institute of Medical Science, University of Tokyo, Tokyo 108-8639, Japan[3]*

The Epstein-Barr virus (EBV)-encoded leader protein, EBNA-LP, strongly activates the EBNA2-mediated transcriptional activation of cellular and viral genes and is therefore important for EBV-induced B-cell transformation. However, a truncated form of EBNA-LP is produced in cells infected with variant EBV strains lacking EBNA2 due to a genetic deletion. The function of this truncated form is unknown. We show here that some Burkitt's lymphoma cells harboring defective EBV strains are specifically resistant to the caspase-dependent apoptosis induced by verotoxin 1 (VT-1) or staurosporine. These cells produced low-molecular-weight Y1Y2-truncated isoforms of EBNA-LP, which were partly localized in the cytoplasm. The transfection of sensitive cells with constructs encoding truncated EBNA-LP isoforms, but not full-length EBNA-LP, induced resistance to caspase-mediated apoptosis. Furthermore, VT-1 induced protein phosphatase 2A (PP2A) activation in sensitive cells but not in resistant cells, in which the truncated EBNA-LP interacted with this protein. Thus, the resistance to apoptosis observed in cells harboring defective EBV strains most probably results from the inactivation of PP2A via interactions with low-molecular-weight Y1Y2-truncated EBNA-LP isoforms.

Epstein-Barr virus (EBV), a gammaherpesvirus, infects human B lymphocytes and can be used to produce immortalized cell lines in vitro. After infection, the viral DNA persists in the cell nucleus, in an episomal form. A limited number of viral proteins are produced, together with two small, noncoding RNAs (EBER1 and EBER2). The viral proteins produced include six EBV nuclear antigens (EBNA1, -2, -3A, -3B, -3C, and EBNA-LP [leader protein]) and three latent membrane proteins (LMP-1, -2A, and -2B) (38, 51). In vivo, EBV can promote the development of several human B-cell cancers, including Burkitt's lymphoma (BL), Hodgkin's lymphoma, and lymphoproliferation, in immunocompromised patients (21). In these EBV-associated B-cell tumors, the latent protein production is highly variable, with some cells producing only EBNA1 (latency I BL) and others expressing the full spectrum of latent EBV genes (posttransplant lymphoma).

The roles of the latent proteins in the development of EBV-associated cancers have been extensively studied. EBNA1 is needed for the maintenance and replication of the EBV episomal genome and is also, apparently, able to inhibit apoptosis (19). EBNA2, -3A, and -3C and LMP-1 are crucial for B-cell transformation in vitro and have antiapoptotic properties, whereas LMP-2A is not essential for cell transformation but provides an important survival signal for B cells (21, 50, 51). EBNA-LP is important for B lymphocyte immortalization by EBV and is a coactivator of EBNA-2-mediated transcriptional activation. However, the gene encoding this protein remains one of the most enigmatic viral genes expressed in infected cells.

The EBNA-LP open reading frame consists of the repeating W1 and W2 exons of the major internal repeat region (IR1) of the EBV genome and the unique C-terminal Y1 and Y2 exons located just downstream from IR1 (39, 43). Due to variations of IR1 in different viruses and alternative splicing between the repeated W1W2 exons and the unique Y1Y2 exons, various isoforms of EBNA-LP are produced in EBV-infected cells (38). Furthermore, a Y1Y2-truncated form of EBNA-LP also exists in cells infected with a variant EBV strain (35). EBNA-LP is found predominantly in the nucleus, but its distribution is variable: it is found in promyelocytic leukemia nuclear bodies (PML NB; multiprotein nuclear structures involved in various cellular processes, including transcriptional regulation, DNA repair, and apoptosis) in lymphoblastoid cell lines, but is distributed diffusely throughout the nucleus in some BL cells or during the early infection of B lymphocytes (30, 44). Furthermore, in cells transfected with a vector encoding EBNA-LP with only one W1W2 repeat, the protein is found exclusively in the cytoplasm (15, 34).

EBNA-LP is known to enhance the EBNA2-mediated transcriptional activation of various cellular (cyclin D2) and viral (LMP-1 and LMP-2B) genes (10, 30, 31, 33, 42). Three functionally conserved regions (CR1, CR2, and CR3) have been identified in the W1W2 domains: CR1 and CR2 constitute a bipartite nuclear localization signal, which, together with CR3, is critical for the transcriptional coactivation function of EBNA-LP. Only proteins with two or more copies of W1W2 display coactivation (28, 34). Studies with recombinant EBV strains containing a Y1Y2-truncated form of EBNA-LP have

---

* Corresponding author. Mailing address: CNRS UMR 8126, Institut Gustave Roussy, Rue Camille Desmoulins, 94805 Villejuif cedex, France. Phone: 33 1 42 11 47 40. Fax: 33 1 42 11 54 94. E-mail: wiels@igr.fr.

shown that this domain plays a role in determining immortalization efficiency but is not required for cooperation with EBNA2 (10, 26, 30). Ling et al. recently showed that EBNA-LP interacts (through the CR3 region) with the PML NB-associated protein Sp100 and that—due to its ability to displace Sp100 and heterochromatin protein 1α from PML NB—this interaction is important for the EBNA-LP coactivation function (25). These data identify, for the first time, some of the components of the PML NB involved in the ability of EBNA-LP to coactivate EBNA2, but the exact mechanism underlying this process still remains to be fully characterized.

EBNA-LP has also been shown to interact with several cellular proteins, including oncogenes and tumor suppressors (pRb, p53, p14ARF, and Fte1/S3a), heat shock proteins (hsp70 and hsp72/hsc73), molecules involved in cell cycle regulation (DNA-PKcs and HA95) and HAX-1, an antiapoptotic protein (6, 9, 14, 15, 27, 45). However, the roles of most of these interactions remain to be established.

We show here that most BL cells containing defective EBV strains are specifically resistant to the caspase-dependent apoptosis induced by verotoxin 1 (VT-1) or staurosporine. These cells produce low-molecular-weight Y1Y2-truncated isoforms of EBNA-LP, which are partly localized in the cytoplasm. The transfection of these truncated EBNA-LP isoforms, but not of full-length molecules, conferred resistance to caspase-mediated apoptosis. VT-1 induced activation of the serine-threonine protein phosphatase 2A (PP2A) in sensitive but not in resistant cells, in which truncated EBNA-LP interacted with this phosphatase. A specific PP2A inhibitor decreased VT-1-induced apoptosis. Thus, the resistance to apoptosis observed in cells containing defective EBV strains probably results from the functional inactivation of PP2A through interaction with Y1Y2-truncated EBNA-LP isoforms.

MATERIALS AND METHODS

Cell lines. All cell lines, except MCF7, were originally established from endemic or sporadic cases of BL. BL70/P3HR1, BL2/P3HR1, and EHRB/Ramos were generated by stable infection of the original EBV-negative BL cell lines with the P3HR1 virus strain, and BL2/B95 was generated by stable infection with the B95-8 virus strain. Sal-BL (EBV$^+$), Oku-BL (EBV$^+$), Oku-BL clone 1, and Oku-BL clone 4 were established at A. Rickinson's laboratory (18). These cell lines were cultured in RPMI 1640 medium (Invitrogen) containing 2 mM L-glutamine, 1 mM sodium pyruvate, 20 mM glucose, 100 U/ml penicillin, and 100 μg/ml streptomycin and supplemented with 10% heat-inactivated fetal calf serum (complete RPMI medium). The MCF7 cell line was cultured in Dulbecco's modified Eagle's medium (DMEM) containing 20 μg/ml gentamicin and supplemented with 10% heat-inactivated fetal calf serum (complete DMEM).

Antibodies and reagents. Purified recombinant VT-1 was kindly provided by C. Lingwood (Toronto, Canada), anti-EBNA-LP monoclonal antibody (MAb) clone 4D3 (40) by Y. Kawagushi (Tokyo, Japan), and anti-EBNA1 MAb clone 1H4 (7) by F. Grasser (Munich, Germany). Staurosporine was obtained from Calbiochem and okadaic acid from Sigma. Anti-caspase 8 MAb (clone 1-3) and anti-poly(ADP-ribose) polymerase (PARP) MAb (Ab-2, clone c-2-10) were purchased from Calbiochem, anti-LMP-1 MAb (CS.1-4) from DAKO, anti-topoisomerase II MAb (Ki-S1) from Chemicon International, anti-EBNA2 (clone PE2) from Novocastra Laboratories, and anti-IκBα MAb (H-4) and goat anti-PP2Ac polyclonal Ab from Santa Cruz Biotechnology, Inc. Horseradish peroxidase (HRP)-conjugated rabbit anti-mouse immunoglobulin G (IgG) (RAM-IgG) and donkey anti-goat Ig (DAG-Ig) were purchased from Zymed Laboratories, Inc., and Santa Cruz Biotechnology, Inc., respectively. Alexa 488-conjugated goat anti-mouse Ig (GAM-Alexa 488) Ab was obtained from Molecular Probes.

Plasmids and transfection. The W1W2Y1Y2, (W1W2)$_2$, (W1W2)$_4$, (W1W2)$_2$Y1Y2, and (W1W2)$_4$Y1Y2 plasmids used in this study were generated as previously described (30). pSG5-LP and pSG5-LPd45 (EBNA-LP lacking the 45

C-terminal codons corresponding to the Y1Y2 domain) plasmids were kindly provided by C. W. Peng (Brigham and Women's Hospital, Harvard University, Boston, MA) and were originally described by Harada et al. (10). For transient transfection experiments, 6×10^5 MCF7 cells were seeded in 24-well plates the day before transfection and 75 to 90% confluent cells were transfected with 3 μg of various plasmids by using Lipofectamine 2000 (Invitrogen) according to the manufacturer's protocol. Six hours after transfection, the cells were washed and placed in fresh complete DMEM. The cells were harvested 48 h after transfection and used for further experiments.

For stable transfection experiments, 10^7 Ramos cells were electroporated (950 μF and 200 mV) with 15 μg pSG5 vector and 3 μg of pSG5(Neo^R); 10 μg of pSG5-LP and 2 μg of pSG5(Neo^R); or 15 μg of pSG5-Ld45 and 3 μg of pSG5(Neo^R). After 48 h, the transfected cells were distributed in 96-well plates (2,000 cells per well) and maintained in complete RPMI 1640 supplemented with 1.6 mg/ml neomycin (PAA Laboratories) for selection. The plates were incubated for 4 weeks, and stable transfectants were then used for further experiments.

Induction of apoptosis and cell death measurement. We incubated 1×10^6 cells for various periods of time at 37°C with either VT-1 (5 ng/ml) or staurosporine (2.5 μM) in 1 ml of complete RPMI medium. The cells were washed in phosphate-buffered saline (PBS), resuspended in annexin buffer (10 mM HEPES-NaOH, pH 7.4, 150 mM NaCl, 5 mM KCl, 1 mM MgCl$_2$, 1.8 mM CaCl$_2$) containing 2.5 μg/ml fluorescein isothiocyanate (FITC)-labeled annexin V (Roche Applied Science), and incubated at 4°C for 5 to 10 min. The cells were washed, resuspended in annexin buffer supplemented with propidium iodide (PI) (10 μg/ml), and analyzed by flow cytometry (FACSCalibur, Becton-Dickinson). Alternatively, levels of cell death were assessed by measuring the proportion of sub-G$_1$ hypodiploid cells. The cells were fixed by incubation in 70% ethanol at −20°C for at least 30 min, washed twice in PBS, and incubated for 30 min at 37°C in 20 mM EDTA, 100 μg/ml RNase A (Sigma-Aldrich, France) and 10 μg/ml PI in PBS. The DNA contents were measured by flow cytometry.

Western blot analysis. A pellet containing 1×10^6 cells was solubilized by incubation in ice-cold lysis buffer (25 mM Tris HCl, pH 6.8, 1% sodium dodecyl sulfate, 50 mM dithiothreitol, complete protease inhibitor) for 10 min. Sample loading buffer (60 mM Tris-HCl, 3% sodium dodecyl sulfate, 10% glycerol, 5% β-mercaptoethanol) was added, and the mixture was boiled for 5 min. The proteins were separated by electrophoresis in 12% bis–Tris precast gels and transferred to polyvinylidene difluoride (PVDF) membranes (Millipore). The blots were blocked overnight at 4°C in 3% nonfat milk powder and 2% glycine in PBS and incubated for 1 h at room temperature with primary antibodies. The blots were washed and incubated with HRP-conjugated RAM-IgG or HRP-conjugated DAG-Ig. The antibody complexes were detected by enhanced chemiluminescence (Amersham Biosciences).

Immunoprecipitation. We disrupted 5×10^6 cells by sonication (10 s on ice) in 1 ml of lysis buffer (150 mM NaCl, 50 mM Tris, pH 7.5, 5 mM EDTA, 0.5% NP-40, 0.5% sodium deoxycholic acid, 0.5% sodium dodecyl sulfate, complete protease inhibitor cocktail). The lysates were mixed with 1 μg of 4D3 anti-EBNA-LP MAb and incubated overnight at 4°C under rotation and then for 4 h at 4°C with 30 μl of protein A-Sepharose beads (Amersham Biosciences). The beads were washed twice with ice-cold lysis buffer and twice with PBS and resuspended in loading buffer. Samples were boiled for 5 min and analyzed by Western blotting.

Preparation of nuclear and cytoplasmic fractions. The cells (1×10^7) were washed, resuspended in ice-cold, low-salt buffer (10 mM Tris, pH 8, 1.5 mM MgCl$_2$, complete protease inhibitor cocktail) and incubated for 10 min at 4°C. They were then centrifuged at $800 \times g$ for 10 min. The cytoplasmic fractions (supernatants) were stored at −80°C, whereas the pellets were resuspended in high-salt buffer (10 mM Tris, pH 8, 1.5 mM MgCl$_2$, 0.5 M NaCl, complete protease inhibitor cocktail) and incubated for 30 min at 4°C. The lysates were centrifuged at $15,000 \times g$ for 15 min and the supernatants—containing the nuclear fractions—were stored at −80°C.

Immunofluorescence. Cells grown on glass coverslips were fixed by incubation in methanol-acetone (1:1) for 10 min at −20°C, washed with PBS, and incubated for 1 h at room temperature with 2% bovine serum albumin in PBS to block nonspecific binding. The cells were then probed with 4D3 anti-EBNA-LP MAb and GAM-Alexa 488 and analyzed by using a Zeiss LSM 510 confocal microscope.

PP2A assay. Cells (3×10^7) were incubated with VT-1 (5 ng/ml) in 30 ml of complete RPMI medium for various periods of time at 37°C. They were washed with Tris-buffered saline, lysed in 300 μl of ice-cold IH buffer (20 mM imidazole-HCl, 2 mM EDTA, 2 mM EGTA, pH 7, 10 μg/ml each of aprotinin, leupeptin, and pepstatin, 1 mM benzamidine, and 1 mM phenylmethylsulfonyl fluoride) and sonicated for 10 s at 4°C. The PP2A immunoprecipitation assay was carried out as recommended by the manufacturer (Upstate). Briefly, subunit C (catalytic) of
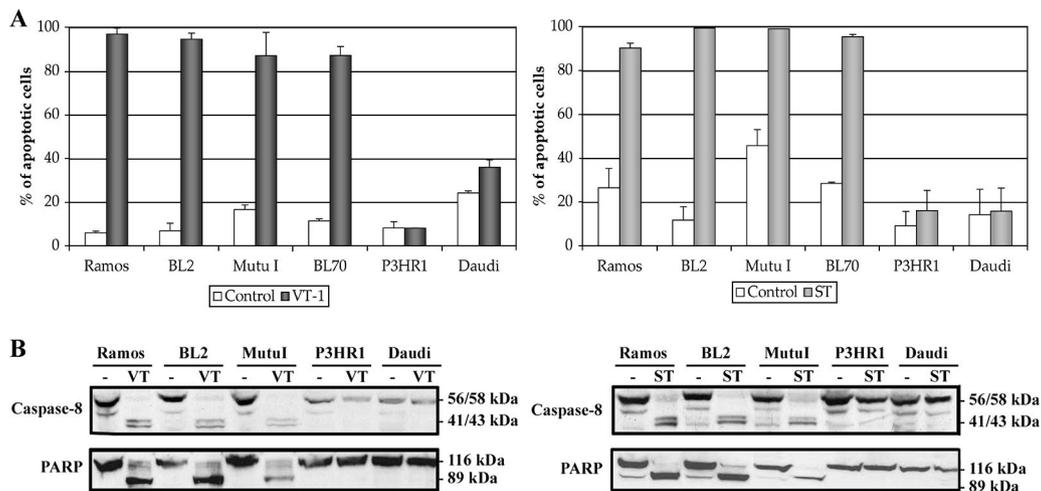
FIG. 1. VT-1 and staurosporine induce caspase-dependent apoptotic cell death in some, but not all, BL cell lines. (A) Cells were incubated for 16 h with VT-1 (5 ng/ml), staurosporine (2.5 μM), or complete RPMI medium (control). The cells were labeled with annexin V-FITC and PI and analyzed with a FACSCalibur flow cytometer to determine the percentages of apoptotic cells. Error bars show the standard deviations. (B) Cells were incubated for 16 h with VT-1, staurosporine, or complete RPMI medium (−). Cell pellets were lysed and equal amounts of protein were subjected to electrophoresis in 12% bis–Tris precast gels. The proteins were transferred to PVDF membranes, which were probed with an anti-caspase 8 MAb or an anti-PARP MAb. Molecular sizes are indicated to the right of each gel.

PP2A was immunoprecipitated and the precipitates were washed twice in lysis buffer and twice in a serine/threonine assay buffer (100 μM $CaCl_2$ and 50 mM Tris-HCl [pH 7.0]). The pellets were resuspended in assay buffer, and the levels of PP2A activity were measured after adding 250 μM phosphopeptide. The phosphatase reactions were allowed to proceed for 10 min at 30°C. The release of phosphate from the added phosphopeptide was quantified with malachite green reagent. Changes in absorbance were measured at 620 nm in a Multiskan EX plate reader (Thermo Electron). A phosphate standard curve for quantifying the levels of phosphatase activity of the samples was generated in parallel.

RESULTS

Burkitt cells containing a defective EBV strain are resistant to caspase-dependent apoptosis. We previously showed that P3HR1 cells were resistant to VT-1-induced apoptosis (48), despite expressing high levels of the VT-1-receptor (the Gb3/CD77 glycolipid antigen). We investigated the mechanism underlying this resistance by assessing the sensitivity to VT-1 of a selected panel of cell lines expressing similar levels of Gb3/CD77 antigen (Fig. 1A, left panel). Four cell lines (Ramos, BL2, Mutu I, and BL70) were highly sensitive to VT-1-induced apoptosis, whereas two others (P3HR1 and Daudi) were completely resistant. VT-1 induced a caspase- and mitochondrion-dependent pathway in sensitive cell lines: caspase 8 activation and the cleavage of PARP (a direct target of caspase 3) were demonstrated by Western blotting (Fig. 1B, left panel), and a loss of mitochondrial membrane potential ($\Delta\psi_m$) was detected by flow cytometry using $DiOC_6(3)$ dye (data not shown). No caspase 8 activation, PARP cleavage, or loss of $\Delta\psi_m$ was observed in the VT-1-resistant cell lines.

P3HR1 and Daudi cells are resistant to VT-1-induced apoptosis but are killed by a caspase-independent pathway induced by anti-Gb3/CD77 MAb (46, 48), suggesting that the resistance mechanism is specific for apoptosis pathways involving caspases. We tested this hypothesis by treating the same cell lines with staurosporine, a kinase inhibitor that induces apoptosis in a caspase-dependent manner (47). The cell viability and levels of caspase activation were assessed. Results

similar to those for VT-1 were obtained: Ramos, BL2, and Mutu I underwent apoptosis, whereas P3HR1 and Daudi did not (Fig. 1A, right panel); caspase 8 activation and PARP cleavage were detected in sensitive cells but not in resistant cells (Fig. 1B, right panels).

The two African BL cell lines, P3HR1 and Daudi, both contain EBV strains lacking the EBNA2 gene and part of the EBNA-LP gene (13, 35). They display an atypical form of latency ("BamHI W promoter [Wp]-restricted"), in which the Wp, rather than the Qp, is active, leading to the production of EBNA1, the EBNA3s, and truncated EBNA-LP (16, 18). We investigated whether this characteristic was involved in the resistance to apoptosis by treating EBV-negative BL cells and their in vitro EBV-infected counterparts with VT-1 or staurosporine. The infection of Ramos, BL2, and BL70 cells with the P3HR1 virus strain (which did not modify Gb3/CD77 expression on the cell surface [data not shown]) strongly decreased sensitivity to VT-1, whereas the infection of BL2 cells with the B95-8 virus strain had only a slight effect (Fig. 2A, left panel). Similarly, Ramos, BL2, and BL70 cells infected with the P3HR1 strain became less sensitive to staurosporine than their EBV-negative parental cells, whereas BL2/B95 cells remained as sensitive as the BL2 cells (Fig. 2A, right panel). The levels of caspase activation were also measured by Western blotting of extracts of treated EBV-negative and EBV-infected cells. Procaspase 8 and PARP were cleaved in Ramos, BL2, and BL2/B95 cells treated with VT-1 or staurosporine but were not cleaved (or only partly cleaved) in EHRB/Ramos and BL2/P3HR1 cells treated with these two compounds (Fig. 2B).

Thus, infection of the cells with a variant EBV strain lacking the EBNA2 gene and the last two coding exons of the EBNA-LP gene seems to protect against the most widely used apoptotic pathway. This protection occurs at the early stages of apoptosis, as caspase 8 showed little or no activation.

Apoptosis-resistant cells produce a truncated, low-molecular-weight EBNA-LP protein, localized in the cytoplasm. As
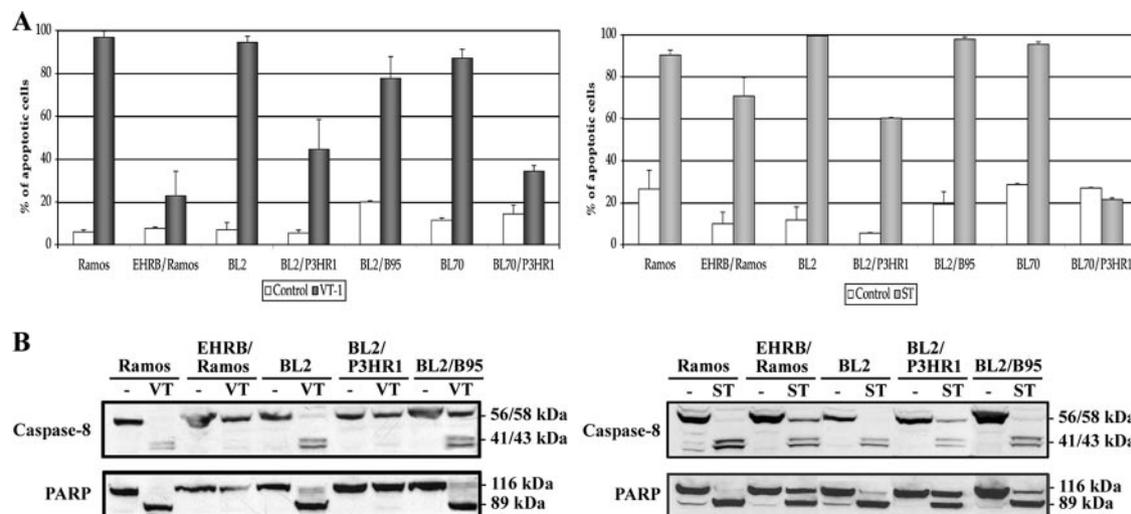
FIG. 2. Infection with the P3HR1 strain of EBV protects BL cells against VT-1- and staurosporine-induced apoptosis. (A) Cells were incubated for 16 h with VT-1 (5 ng/ml), staurosporine (2.5 μM), or complete RPMI medium (control). The cells were labeled with annexin V-FITC and PI and analyzed with a FACSCalibur flow cytometer to determine the percentages of apoptotic cells. Error bars show the standard deviations. (B) Cells were incubated for 16 h with VT-1, staurosporine, or complete RPMI medium (−). Cell pellets were lysed, and equal amounts of protein were subjected to electrophoresis in 12% bis–Tris precast gels. The proteins were transferred to PVDF membranes, which were probed with an anti-caspase 8 MAb or an anti-PARP MAb. Molecular sizes are indicated to the right of each gel.

VT-1 and staurosporine induce apoptosis in EBV-negative BL cells, resistance to apoptosis is unlikely to be due to the lack of EBNA2 in P3HR1-infected cells. We therefore hypothesized that the truncated form of EBNA-LP might be involved in this resistance. EBNA-LP is variable in size, even when not truncated, and its location, in the nucleus or cytoplasm, depends on the number of W1W2 repeats. We first investigated the production and size of the EBNA-LP protein in sensitive and resistant cell lines. Western blot analysis was performed with the 4D3 anti-EBNA-LP MAb, which has been shown to react with all isoforms of EBNA-LP protein (40). EBNA-LP was detected as a 27-kDa band in the P3HR1, EHRB/Ramos, and BL2/P3HR1 extracts (with a minor band at 50 kDa in BL2/P3HR1), as a 34-kDa band in the Daudi extract, and as a 70-75-kDa doublet band in the BL2/B95 extract. Ramos and BL2 cells, which are EBV negative, and Mutu I cells, a BL cell line with a group I phenotype (8), did not produce EBNA-LP (Fig. 3A). Thus, cells resistant to VT-1- or staurosporine-induced apoptosis contain a low-molecular-weight, truncated EBNA-LP protein, whereas sensitive cells contain either a high-molecular-weight, full-length EBNA-LP protein or no EBNA-LP. As other latent EBV proteins are known to protect cells against apoptosis (19, 23, 24), we assessed the levels of these proteins in our cell lines. As expected, all EBV-positive cells expressed EBNA1 (although at different levels and with slightly different molecular weights), and only BL2/B95 cells expressed EBNA2 and LMP-1 (Fig. 3A). The lack of correlation between the expression of these EBV latent proteins and the resistance to VT-1- or staurosporine-induced apoptosis observed in P3HR1-infected cells indicate that these proteins are not involved in this phenomenon.

We further investigated the possible role of the truncated EBNA-LP protein in resistance to apoptosis by determining its subcellular distribution. Protein extracts were separated into nuclear and cytoplasmic fractions, and Western blotting was

performed with 4D3 anti-EBNA-LP MAb. We checked the quality of fractionation by also probing blots with antibodies recognizing proteins known to be localized in the nucleus (topoisomerase II) or in the cytoplasm (IκBα). The 27-kDa and 34-kDa forms of EBNA-LP, expressed in P3HR1, EHRB/Ramos, BL2/P3HR1, and Daudi cells, were found only or mostly in the cytoplasmic fractions, whereas the minor, 50-kDa band expressed in BL2/P3HR1 cells was found in the nuclear fraction. By contrast, the 70-75-kDa doublet detected in the BL2/B95 extract was strictly nuclear (Fig. 3B).

BL cell lines (Sal-BL and Oku-BL) carrying both a viral genome with a deletion (e.g., P3HR1 and Daudi) and a wild-type genome, but in which only the genome with a deletion is expressed, have recently been established (16, 18). The production and distribution of EBNA-LP were investigated in these cell lines and in subclones of Oku-BL containing either both genomes (clone 4) or only the genome with a deletion (clone 1) (18). EBNA-LP was detected as a single, predominantly nuclear, 50-kDa band in Sal-BL cells. Various isoforms (35, 47, and 80 kDa) were present in Oku-BL extracts, and these isoforms were also predominantly nuclear. These isoforms were not detected in the subclones, but a 150-kDa band, equally distributed between the cytoplasm and nucleus, was detected in Oku-BL clone 1, whereas a faint, 27-kDa band (similar to that in P3HR1 cells) was detected in the cytoplasmic fraction of Oku-BL clone 4 (Fig. 3C). We assessed the sensitivity of these cell lines to staurosporine and VT-1. Staurosporine induced apoptosis in 60% of Sal-BL, Oku-BL, and Oku-BL clone 1 cells, whereas only 36% of Oku-BL clone 4 cells were killed by this compound; similar results were obtained with VT-1, with Oku-BL clone 4 cells being more resistant than the other cells (Table 1).

Thus, cells resistant to caspase-dependent apoptosis seem to contain a truncated, low-molecular-weight EBNA-LP protein, localized predominantly in the cytoplasm (P3HR1 [parental or
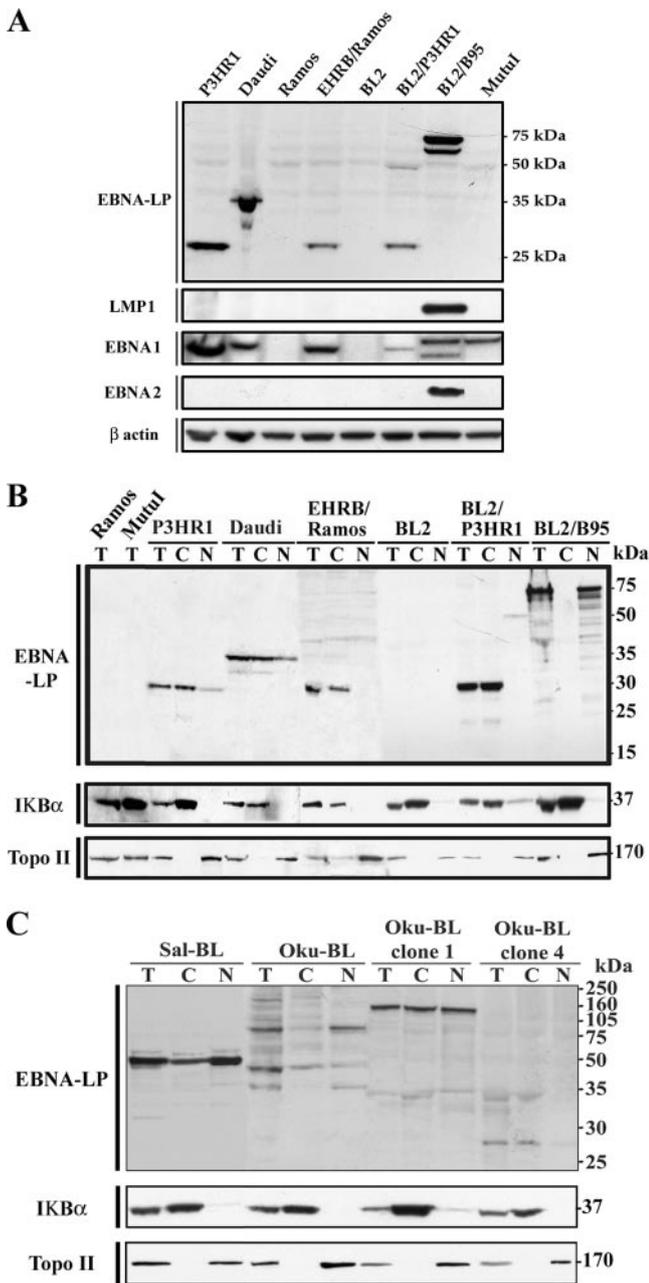
A

B

C

FIG. 3. Levels of expression of various EBV latent proteins and subcellular distributions of EBNA-LP in various BL cell lines and derived cell clones. (A) Cell pellets were lysed and equal amounts of protein were subjected to electrophoresis in 12% bis–Tris precast gels. The proteins were transferred to PVDF membranes, which were probed with 4D3 anti-EBNA-LP MAb, CS.1-4 anti-LMP-1 MAb, 1H4 anti-EBNA1 MAb, PE2 anti-EBNA2 MAb, or an anti-β-actin MAb (as a control for protein loading). (B and C) Total lysates (T) were fractionated into cytoplasmic (C) and nuclear (N) extracts. Equal amounts of each fraction (20 μg protein) were subjected to electrophoresis in 12% bis–Tris precast gels. The proteins were transferred to PVDF membranes, which were probed with 4D3 anti-EBNA-LP MAb. We checked that fractionation was complete by probing the membranes with MAbs recognizing a nuclear protein (topoisomerase II) and a cytoplasmic protein (IκBα). Molecular sizes are indicated to the right.

TABLE 1. VT-1- and staurosporine-induced apoptosis in Oku-BL cells and derived cell clones[a]

Cell line	% Apoptotic cells (± SD) with:		
	Control	Staurosporine	VT-1
Oku-BL	17 ± 8	63 ± 9	69 ± 2
Oku clone 1	19 ± 10	60 ± 10	72 ± 1
Oku clone 4	18 ± 9	36 ± 7	52 ± 1
Sal-BL	20 ± 2	61 ± 2	81 ± 1

[a] The cells were incubated for 16 h with VT-1 (5 ng/ml), staurosporine (2.5 μM), or complete RPMI medium (control). The cells were labeled with annexin V-FITC and PI and analyzed with a FACSCalibur flow cytometer to determine the percentages of apoptotic cells.

converted cells], Daudi, and Oku-BL clone 4), whereas sensitive cells produce either a full-length high-molecular-weight protein (BL2/B95) or a truncated high-molecular-weight protein localized predominantly in the nucleus (Sal-BL, Oku-BL, and Oku-BL clone 1).

Transfection with a Y1Y2-truncated EBNA-LP construct protects cells against caspase-dependent apoptosis. We used transient and stable transfection experiments to investigate the roles of various truncated and full-length isoforms of EBNA-LP in resistance to apoptosis. As BL cells have a very low transfection efficiency, we used MCF7 cells (which regularly yielded 80% transfected cells) for transient transfection with various pSG5-based EBNA-LP constructs. On Western blots, the (W1W2)$_4$Y1Y2 construct gave a 37-kDa protein, (W1W2)$_4$ a 32-kDa protein, (W1W2)$_2$Y1Y2 a 22-kDa protein, (W1W2)$_2$ a 17-kDa protein, and (W1W2)$_1$Y1Y2 a 16-kDa protein (Fig. 4A). The subcellular distributions of the variant EBNA-LP proteins in the transiently transfected cells were assessed by confocal microscopy (Fig. 4B). Full-length EBNA-LP, with two or four W1W2 repeats, was detected only in cell nuclei [with, however, faint cytoplasmic staining also observed with the (W1W2)$_4$Y1Y2 construct], whereas the protein with only one repeat was found exclusively in the cytoplasm (detected as numerous large spots). Y1Y2-truncated EBNA-LP with two or four W1W2 repeats was found either in the nuclei only or in both the nuclei and cytoplasm. In this case, the cytoplasmic staining was diffuse and usually weaker than the nuclear staining (see the high-magnification image of cells transfected with the construct containing four W1W2 repeats).

As MCF7 cells do not express the Gb3/CD77 antigen, we assessed the sensitivity of transfectants to apoptosis by treating them with staurosporine only. We quantified apoptosis by measuring the percentages of cells in the sub-G$_1$ fractions, and the inhibition of apoptosis was determined by comparison with cells transfected with the empty pSG5 vector. Full-length EBNA-LP [(W1W2)$_4$Y1Y2 and (W1W2)$_2$Y1Y2] conferred slight protection against staurosporine (16% ± 5% and 24% ± 1% inhibition of apoptosis, respectively), whereas the Y1Y2-truncated EBNA-LP, although produced in smaller amounts than the full-length proteins [compare (W1W2)$_4$ with (W1W2)$_4$Y1Y2 and (W1W2)$_2$ with (W1W2)$_2$Y1Y2 in Fig. 4A], had a much stronger effect [58% ± 3% and 57% ± 6% inhibition for the (W1W2)$_4$ and (W1W2)$_2$ constructs, respectively]. Interestingly, the full-length protein with only one W1W2 repeat conferred intermediate protection (36% ± 4% inhibition of apoptosis) (Fig. 4C).
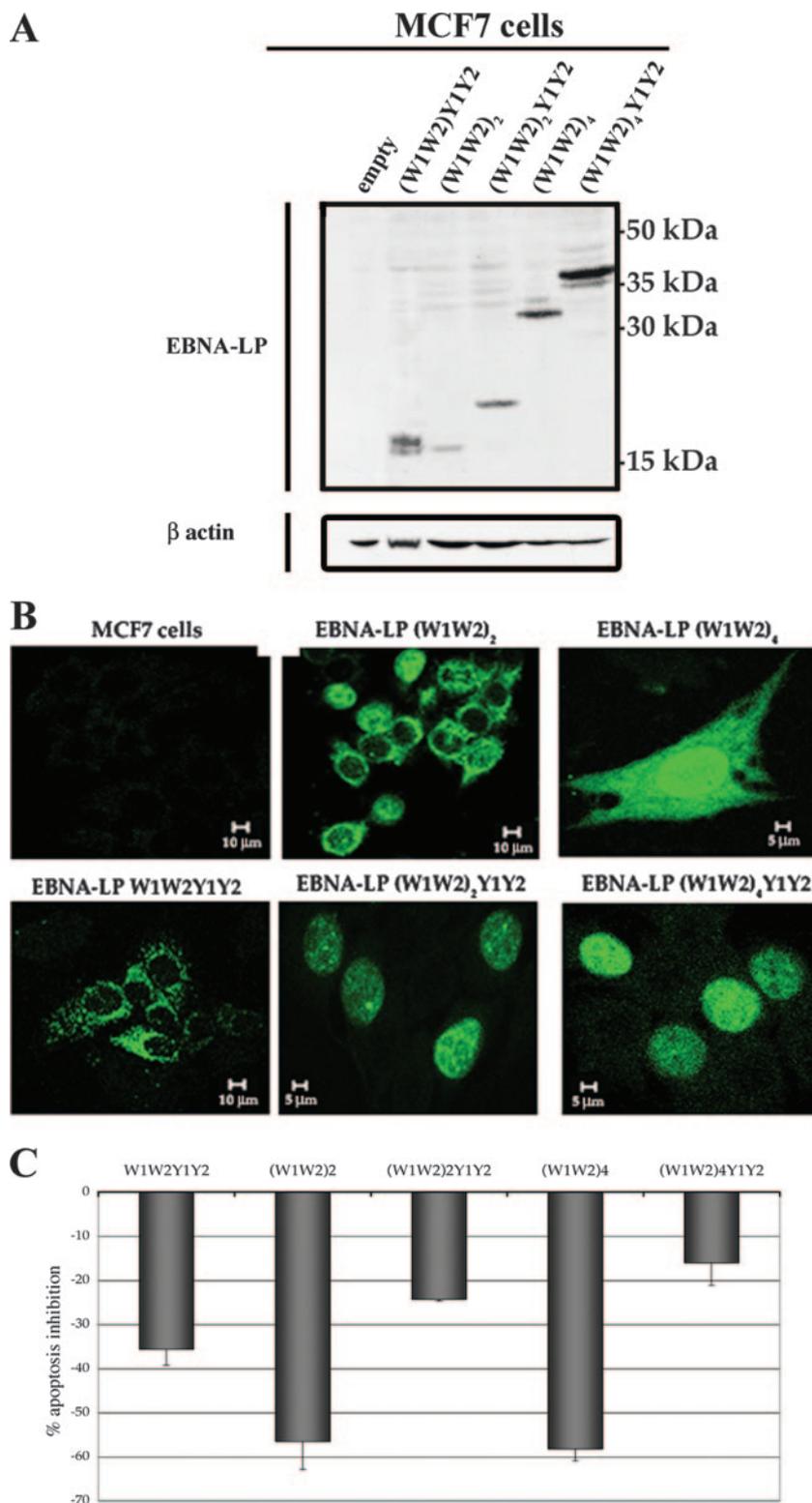
FIG. 4. Production levels, subcellular distributions, and effects on apoptosis of EBNA-LP after transient transfection. (A) MCF7 cells were transfected with 3 μg of various EBNA-LP expression vectors and grown for 48 h. Cell pellets were lysed, and equal amounts of protein were subjected to electrophoresis in 12% bis–Tris precast gels. The proteins were transferred to PVDF membranes, which were probed with 4D3 anti-EBNA-LP MAb or an anti-β-actin MAb (as a control for protein loading). Molecular sizes are indicated to the right. (B) MCF7 cells were transfected with 3 μg of various EBNA-LP expression vectors and grown on glass coverslips; 48 h after transfection, the cells were stained with 4D3 anti-EBNA-LP MAb and GAM-Alexa 488. (C) MCF7 cells were transfected with 3 μg of various EBNA-LP expression vectors; 48 h after transfection, the cells were treated with staurosporine (2.5 μM) for 6 h and stained with PI. The levels of apoptosis were assessed by determining the proportions of cells with sub-G_1 DNA content by flow cytometry. The percentages of apoptosis inhibition were determined by comparison with cells transfected with the pSG5 vector. Error bars show the standard deviations.
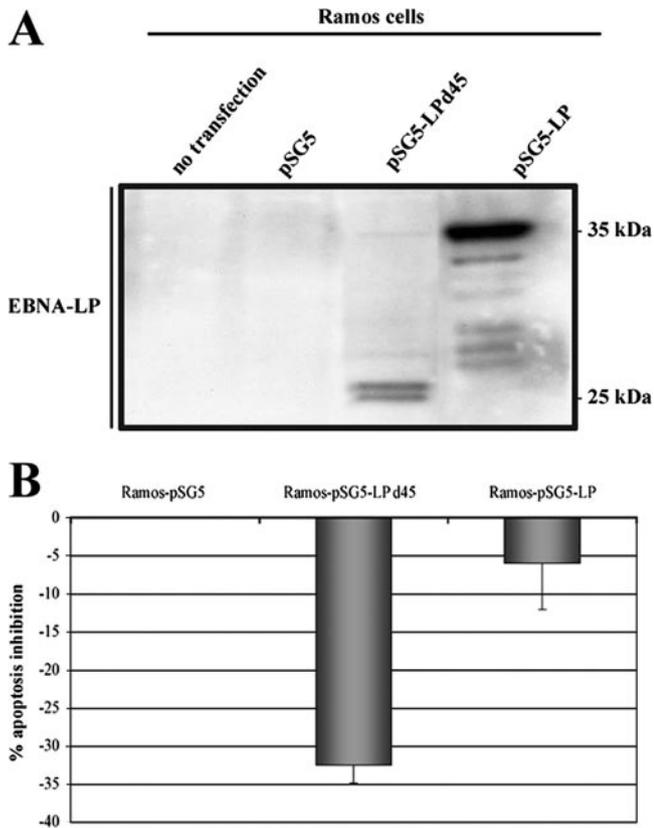
A

Ramos cells

EBNA-LP

35 kDa

25 kDa

B

FIG. 5. Effect of stable transfection of EBNA-LP on apoptosis. Ramos cells were cotransfected with EBNA-LP expression vectors and the pSG5(Neo^R) vector, which carries the neomycin resistance gene. The cells were grown in selection medium (complete RPMI supplemented with 16 mg/ml neomycin) for 4 weeks, and the clones were then tested. (A) Cell pellets were lysed, and equal amounts of protein were subjected to electrophoresis in 12% bis–Tris precast gels. The proteins were transferred to PVDF membranes, which were probed with 4D3 anti-EBNA-LP MAb. Molecular sizes are indicated to the right. (B) Stable transfectants were treated with VT-1 (5 ng/ml) for 16 h, labeled with annexin V-FITC and PI, and analyzed by using a FACScalibur flow cytometer to determine the percentages of apoptotic cells. The percentages of apoptosis inhibition were determined by comparison with cells transfected with the pSG5 vector. Error bars shown the standard deviations.

For confirmation of these results, we also derived Ramos cells that stably expressed full-length or Y1Y2-truncated EBNA-LP. The EBNA-LP expression levels were checked by Western blot analysis (Fig. 5A), and the sensitivity to apoptosis of these stable transfectants were determined by treating them with VT-1 (Fig. 5B). Compared to cells transfected with the empty pSG5 vector, cells expressing full-length EBNA-LP (Ramos-pSG5-LP) were not resistant to apoptosis ($6.5\% \pm 6\%$ inhibition of apoptosis), whereas cells expressing Y1Y2-truncated EBNA-LP (Ramos-pSG5-LPd45) displayed significant protection against the effects of VT-1 ($32.5\% \pm 2\%$ inhibition of apoptosis).

These results confirm our previous observations and demonstrate that truncated and cytoplasmic EBNA-LP protects cells against caspase-dependent apoptosis.

PP2A is involved in the apoptotic signaling cascade and forms a complex with EBNA-LP in resistant cells. PP2A regulates several apoptotic signaling pathways at the level of or
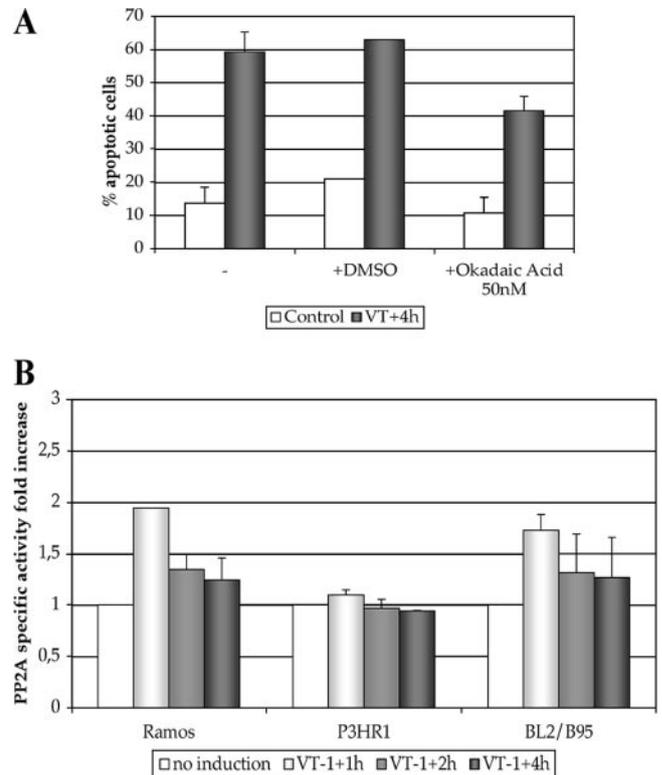
A

B

FIG. 6. PP2A is involved in VT-1-induced apoptosis. (A) Ramos cells were incubated with okadaic acid (50 nM) or with vehicle (DMSO) or without any treatment (−) for 1 h before being treated with VT-1 for 4 h. The cells were labeled with annexin V-FITC and PI and analyzed by using a FACScalibur flow cytometer to determine the percentages of apoptotic cells. (B) VT-1-sensitive or -resistant cells were incubated with or without VT-1 (5 ng/ml) for various periods of time and lysed. The lysates were immunoprecipitated with an anti-PP2A Ab, and the levels of PP2A activity were determined by measuring the release of phosphate from a phosphopeptide substrate in a colorimetric assay. The increases in the PP2A activity levels of treated samples were determined with respect to the levels in untreated samples. Error bars indicate the standard deviations.

upstream from the initiator caspase 8 (11). We investigated the possible involvement of PP2A in our caspase-dependent apoptotic pathways by using okadaic acid, a potent inhibitor of this phosphatase. Ramos cells, with or without prior incubation with okadaic acid, were treated with VT-1, and the levels of apoptosis were measured. PP2A inhibition significantly decreased the sensitivity to VT-1 ($41\% \pm 4\%$ apoptotic cells in samples treated with okadaic acid versus $63\% \pm 1\%$ in control samples; Fig. 6A), suggesting that this phosphatase is involved in the VT-1-induced signaling cascade.

We then measured the levels of PP2A-specific activity of sensitive (Ramos and BL2/B95) and resistant (P3HR1) cells treated with or without VT-1 for various periods of time. Before treatment, the levels of phosphatase activity of PP2A-immune complexes were similar in all three cell lines (Ramos, 95 pmol phosphate/min/mg protein; BL2/B95, 134 pmol phosphate/min/mg protein; and P3HR1, 103 pmol phosphate/min/mg protein), but marked differences were observed after incubation with VT-1. The levels of PP2A activity increased strongly in both Ramos and BL2/B95 cells after 1 h of treat-
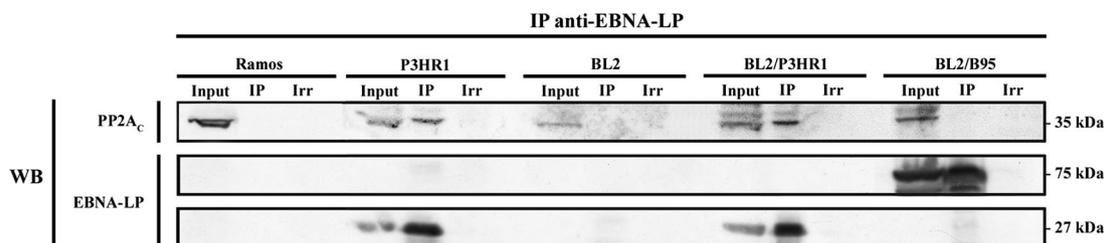
FIG. 7. PP2A interacts with EBNA-LP in cells resistant to VT-1-induced apoptosis. Lysates obtained from various VT-1-sensitive or -resistant cells were subjected to immunoprecipitation (IP) with 4D3 anti-EBNA-LP MAb or irrelevant Abs (Irr). Western blot analysis was then performed with an anti-PP2Ac Ab or 4D3 anti-EBNA-LP MAb. As a control for protein levels before IP, a portion of cell lysate (Input) corresponding to 15% of the input for IP was also included in the Western blot analysis. Molecular sizes are indicated to the right.

ment (factors of 1.9 ± 0.01 and 1.7 ± 0.15, respectively) and then decreased, reaching nearly basal levels after 2 and 4 h. By contrast, the level of PP2A activity of P3HR1 cells was unaffected by VT-1 treatment (Fig. 6B).

Having demonstrated the involvement of PP2A activation in VT-1-induced apoptosis, we investigated whether the truncated, low-molecular-weight EBNA-LP could interfere with PP2A. Coimmunoprecipitation experiments were carried out with P3HR1 and Ramos protein extracts and with BL2, BL2/P3HR1, and BL2/B95 extracts for comparison of cells with the same background. Immunoprecipitations were performed with 4D3 anti-EBNA-LP MAb, and the immunoprecipitates were probed for PP2A. The catalytic subunit of PP2A was detected as a 36-kDa protein in the inputs of all five cell lines and was coprecipitated with the truncated EBNA-LP protein in P3HR1 and BL2/P3HR1 cells, but not with the full-length protein in BL2/B95 cells (Fig. 7). Control Western blots with 4D3 anti-EBNA-LP MAb showed that this molecule was immunoprecipitated in BL2/B95 as a 70-75-kDa doublet and in P3HR1 and BL2/P3HR1 as a 27-kDa band (Fig. 7). The coimmunoprecipitation of PP2A with EBNA-LP did not depend on the amount of EBNA-LP in the cells, because BL2/B95 cells consistently produce larger amounts of this protein than P3HR1 or BL2/P3HR1 (see the inputs of these three cell lines in Fig. 7 and also Fig. 3). We can therefore conclude that the interaction between PP2A and truncated EBNA-LP prevents PP2A activation, resulting in resistance to apoptosis.

DISCUSSION

In this study, we showed that a C-terminally truncated variant viral EBNA-LP protein, lacking the Y1Y2 domains and with a limited number of W1W2 repeats, conferred resistance to caspase-dependent apoptosis by interacting with cellular PP2A. This conclusion is based on the demonstration that EBV-infected BL cells producing low-molecular-weight truncated isoforms of EBNA-LP are not killed by two potent inducers (VT-1 and staurosporine) of caspase-dependent apoptosis, whereas cells producing full-length isoforms are killed. Furthermore, the transient and stable transfection of EBV-negative cells with truncated EBNA-LP strongly decreased their sensitivity to VT-1- and staurosporine-induced apoptosis. Finally, we showed that PP2A was involved in triggering apoptosis, as an inhibitor of this phosphatase significantly reduced cell sensitivity to apoptotic inducers and the levels of PP2A activity increased in sensitive, but not resistant cells,

following treatment with VT-1. We showed, by coimmunoprecipitation, that truncated EBNA-LP interacted specifically with PP2A.

Many studies have investigated the role of EBNA-LP, but most have focused on the full-length protein and its role as a coactivator of EBNA2. This study is the first to demonstrate that the truncated EBNA-LP has a specific function in itself: protecting cells against caspase-dependent apoptosis.

We showed that the subcellular distributions of full-length and truncated EBNA-LP clearly differed. Native truncated EBNA-LP was predominantly localized in the cytoplasm, and the transfected truncated form was found in both nucleus and cytoplasm. By contrast, the full-length protein (native and transfected) was almost exclusively nuclear. However, the localization of the truncated form of the protein also depends on the number of W1W2 repeats. Indeed, the truncated EBNA-LP isoforms expressed by Sal-BL and Oku-BL cells, which have molecular masses above 50 kDa, were found predominantly in the nucleus. The observations that these cells were sensitive to apoptosis and that transfection with a full-length EBNA-LP construct containing only one W1W2 repeat (which localized exclusively in the cytoplasm) conferred to the cells intermediate protection to apoptosis stress the importance of the cytoplasmic localization of the low-molecular-weight, truncated EBNA-LP in the protection against apoptosis.

The cellular distribution of the full-length and truncated EBNA-LP forms has long been a matter of debate. Nitsche et al. (30) reported that Y1Y2-truncated EBNA-LP was present in the nuclei of transfected cells and therefore able to cooperate with EBNA2. However, transfection efficiency was low (10 to 15% of the cells) and few labeled cells were shown. We found that cytoplasmic labeling was weaker than nuclear staining, so the cytoplasmic staining may have been too weak to be detected in Nitsche's study. Although full-length EBNA-LP molecules with two or more W1W2 repeats are generally considered to be localized exclusively in the nucleus, various studies have shown that some of this protein is also detectable in the cytoplasm, where it can interact with HAX-1 (6, 15, 28, 34), a protein involved in apoptosis and cell migration (36, 41). It therefore seems likely that all isoforms of EBNA-LP are present in various ratios in both the nucleus and the cytoplasm, but it remains to be determined whether this distribution is permanent or, as suggested by Peng et al. (34), whether EBNA-LP shuttles between the nucleus and the cytoplasm. Ad-

dressing this issue would provide insight into the functional roles of the various isoforms of EBNA-LP.

We provide evidence that the resistance to apoptosis displayed by cells containing truncated EBNA-LP results from the interaction of this viral protein with PP2A, inhibiting the activity of this phosphatase. EBNA-LP homologs are present in several nonhuman primate lymphocryptoviruses, and five conserved regions have been identified. Three of these regions (CR1, CR2, and CR3) are localized in the W1W2 repeats (32) and were shown to be crucial for the EBNA-LP coactivation function (28, 34). Determining whether the truncated forms of the lymphocryptovirus EBNA-LP homologs also protect cells against caspase-dependent apoptosis and specifically coprecipitate PP2A would provide information about EBNA-LP/PP2A interactions. If this were the case, the introduction of mutations or deletions in the conserved regions would make it possible to identify the functional domains of EBNA-LP interacting with PP2A.

PP2A is a major Ser/Thr cellular phosphatase involved in regulating many processes, including transcription, translation, cell cycle progression, and various signal transduction pathways. The core enzyme is a dimer, consisting of a catalytic subunit (PP2A$_c$) and a regulatory constant subunit (PR65/A). This core dimer can interact with a third variable subunit (B subunit), four families of which have been identified. The association of the core dimer with one of these B subunits may account for the differences in the substrate specificities and regulatory activities of PP2A. PP2A activities are also regulated by interactions with many cellular or viral proteins (12, 22).

PP2A has been reported to be involved in apoptosis, mainly due to its ability to interfere with proteins of the Bcl-2 family (49). PP2A has also been shown to regulate apoptosis by acting on caspases 8 and 3 (2). We are currently measuring the levels of caspase 8 and caspase 3 phosphorylation in our BL cell lines, and we will determine whether the increases in the activity of PP2A observed following the treatment of sensitive cells with VT-1 correlate with changes in these levels. As the apoptotic pathways induced by VT-1 and staurosporine involve mitochondrial depolarization, we will also assess the levels of Bcl-2 and Bax phosphorylation during these processes.

Another viral protein, the small t (ST) antigen of simian virus 40 (SV40), is known to inhibit PP2A activity. SV40 is a DNA tumor virus of the polyomavirus family that has been widely studied. Two proteins from this virus (large T and ST) disturb key tumor suppressor pathways in the cell and play essential roles in the oncogenic properties of this virus (3). PP2A deregulation by ST is absolutely required for the transformation process, and ST specifically targets the B′/B56/PR61 (B56γ) variable subunit (4). In BL cells resistant to VT-1-induced apoptosis, truncated EBNA-LP forms a complex with PP2A$_c$, probably preventing its activation. It remains to be determined whether the association between EBNA-LP and the C subunit is direct or involves the PR65/A subunit and whether this association can displace the various B subunits from the core dimer.

What is the role of the survival advantage conferred by truncated EBNA-LP, particularly in the absence of EBNA2? Early in the infection of primary B lymphocytes with P3HR1, EBNA-LP is the only product detected, whereas infection with B95-8 induces the production of EBNA-LP and EBNA2, followed by EBNA1 and the EBNA3s (1, 37, 42). The early and sustained production of truncated EBNA-LP during the primary infection of tonsillar B cells may enable these cells to resist germinal center selection, which occurs through activation of the caspase-dependent death receptor pathway (5). Interleukin-10, which is produced in germinal centers (29), was recently shown to induce the expression of LMP-1—the major transforming EBV gene product—in tonsillar B cells infected with P3HR1 (20). The survival advantage conferred by the truncated EBNA-LP, combined with the induction of LMP-1 by interleukin-10, may, therefore, favor the production in vivo of immortalized B cells bearing mutant EBV. Perhaps most importantly, the ability to overcome apoptosis conferred by truncated EBNA-LP also constitutes a clear advantage for the development of tumor cells. Recent reports have shown that, among clones of BL cell lines differing in EBV status, those with the "Wp-restricted" latency form (displayed by cells infected with a virus lacking EBNA2) have the highest degree of protection from apoptosis (17, 18). It has been suggested that EBNA3 protein production in these cells is responsible for this protection (18). Our results demonstrate that truncated EBNA-LP may also potentially account for the survival advantage of these cells. Furthermore, the observation that all viruses identified so far with a deletion of EBNA2 have deletions of the EBNA-LP Y1 and Y2 exons provides strong evidence for a specific role for the truncated EBNA-LP protein in the persistence of these mutant viruses.

REFERENCES

1. **Alfieri, C., M. Birkenbach, and E. Kieff.** 1991. Early events in Epstein-Barr virus infection of human B lymphocytes. Virology **181:**595–608.
2. **Alvarado-Kristensson, M., and T. Andersson.** 2005. Protein phosphatase 2A regulates apoptosis in neutrophils by dephosphorylating both p38 MAPK and its substrate caspase 3. J. Biol. Chem. **280:**6238–6244.
3. **Chen, W., and W. C. Hahn.** 2003. SV40 early region oncoproteins and human cell transformation. Histol. Histopathol. **18:**541–550.
4. **Chen, W., R. Possemato, K. T. Campbell, C. A. Plattner, D. C. Pallas, and W. C. Hahn.** 2004. Identification of specific PP2A complexes involved in human cell transformation. Cancer Cell **5:**127–136.
5. **Defrance, T.** 2005. Mature B cells: apoptosis checkpoints. Transplantation **79:**S4–S7.
6. **Dufva, M., M. Olsson, and L. Rymo.** 2001. Epstein-Barr virus nuclear antigen 5 interacts with HAX-1, a possible component of the B-cell receptor signalling pathway. J. Gen. Virol. **82:**1581–1587.
7. **Grasser, F. A., P. G. Murray, E. Kremmer, K. Klein, K. Remberger, W. Feiden, G. Reynolds, G. Niedobitek, L. S. Young, and N. Mueller-Lantzsch.** 1994. Monoclonal antibodies directed against the Epstein-Barr virus-encoded nuclear antigen 1 (EBNA1): immunohistologic detection of EBNA1 in the malignant cells of Hodgkin's disease. Blood **84:**3792–3798.
8. **Gregory, C. D., M. Rowe, and A. B. Rickinson.** 1990. Different Epstein-Barr virus-B cell interactions in phenotypically distinct clones of a Burkitt's lymphoma cell line. J. Gen. Virol. **71:**1481–1495.
9. **Han, I., S. Harada, D. Weaver, Y. Xue, W. Lane, S. Orstavik, B. Skalhegg, and E. Kieff.** 2001. EBNA-LP associates with cellular proteins including DNA-PK and HA95. J. Virol. **75:**2475–2481.
10. **Harada, S., and E. Kieff.** 1997. Epstein-Barr virus nuclear protein LP stimulates EBNA-2 acidic domain-mediated transcriptional activation. J. Virol. **71:**6611–6618.
11. **Harmala-Brasken, A. S., A. Mikhailov, T. S. Soderstrom, A. Meinander,**

T. H. Holmstrom, Z. Damuni, and J. E. Eriksson. 2003. Type-2A protein phosphatase activity is required to maintain death receptor responsiveness. Oncogene 22:7677–7686.

12. Janssens, V., and J. Goris. 2001. Protein phosphatase 2A: a highly regulated family of serine/threonine phosphatases implicated in cell growth and signalling. Biochem. J. 353:417–439.

13. Jones, M. D., L. Foster, T. Sheedy, and B. E. Griffin. 1984. The EB virus genome in Daudi Burkitt's lymphoma cells has a deletion similar to that observed in a non-transforming strain (P3HR-1) of the virus. EMBO J. 3:813–821.

14. Kashuba, E., M. Yurchenko, K. Szirak, J. Stahl, G. Klein, and L. Szekely. 2005. Epstein-Barr virus-encoded EBNA-5 binds to Epstein-Barr virus-induced Fte1/S3a protein. Exp. Cell Res. 303:47–55.

15. Kawaguchi, Y., K. Nakajima, M. Igarashi, T. Morita, M. Tanaka, M. Suzuki, A. Yokoyama, G. Matsuda, K. Kato, M. Kanamori, and K. Hirai. 2000. Interaction of Epstein-Barr virus nuclear antigen leader protein (EBNA-LP) with HS1-associated protein X-1: implication of cytoplasmic function of EBNA-LP. J. Virol. 74:10104–10111.

16. Kelly, G., A. Bell, and A. Rickinson. 2002. Epstein-Barr virus-associated Burkitt lymphomagenesis selects for downregulation of the nuclear antigen EBNA2. Nat. Med. 8:1098–1104.

17. Kelly, G. L., A. E. Milner, G. S. Baldwin, A. I. Bell, and A. B. Rickinson. 2006. Three restricted forms of Epstein-Barr virus latency counteracting apoptosis in c-myc-expressing Burkitt lymphoma cells. Proc. Natl. Acad. Sci. USA 103:14935–14940.

18. Kelly, G. L., A. E. Milner, R. J. Tierney, D. S. Croom-Carter, M. Altmann, W. Hammerschmidt, A. I. Bell, and A. B. Rickinson. 2005. Epstein-Barr virus nuclear antigen 2 (EBNA2) gene deletion is consistently linked with EBNA3A, -3B, and -3C expression in Burkitt's lymphoma cells and with increased resistance to apoptosis. J. Virol. 79:10709–10717.

19. Kennedy, G., J. Komano, and B. Sugden. 2003. Epstein-Barr virus provides a survival factor to Burkitt's lymphomas. Proc. Natl. Acad. Sci. USA 100:14269–14274.

20. Kis, L. L., M. Takahara, N. Nagy, G. Klein, and E. Klein. 2006. IL-10 can induce the expression of EBV-encoded latent membrane protein-1 (LMP-1) in the absence of EBNA-2 in B lymphocytes and in Burkitt lymphoma- and NK lymphoma-derived cell lines. Blood 107:2928–2935.

21. Kuppers, R. 2003. B cells under influence: transformation of B cells by Epstein-Barr virus. Nat. Rev. Immunol. 3:801–812.

22. Lechward, K., O. S. Awotunde, W. Swiatek, and G. Muszynska. 2001. Protein phosphatase 2A: variety of forms and diversity of functions. Acta Biochim. Pol. 48:921–933.

23. Lee, J. M., K. H. Lee, C. J. Farrell, P. D. Ling, B. Kempkes, J. H. Park, and S. D. Hayward. 2004. EBNA2 is required for protection of latently Epstein-Barr virus-infected B cells against specific apoptotic stimuli. J. Virol. 78:12694–12697.

24. Li, H. P., and Y. S. Chang. 2003. Epstein-Barr virus latent membrane protein 1: structure and functions. J. Biomed. Sci. 10:490–504.

25. Ling, P. D., R. S. Peng, A. Nakajima, J. H. Yu, J. Tan, S. M. Moses, W. H. Yang, B. Zhao, E. Kieff, K. D. Bloch, and D. B. Bloch. 2005. Mediation of Epstein-Barr virus EBNA-LP transcriptional coactivation by Sp100. EMBO J. 24:3565–3575.

26. Mannick, J. B., J. I. Cohen, M. Birkenbach, A. Marchini, and E. Kieff. 1991. The Epstein-Barr virus nuclear protein encoded by the leader of the EBNA RNAs is important in B-lymphocyte transformation. J. Virol. 65:6826–6837.

27. Mannick, J. B., X. Tong, A. Hemnes, and E. Kieff. 1995. The Epstein-Barr virus nuclear antigen leader protein associates with hsp72/hsc73. J. Virol. 69:8169–8172.

28. McCann, E. M., G. L. Kelly, A. B. Rickinson, and A. I. Bell. 2001. Genetic analysis of the Epstein-Barr virus-coded leader protein EBNA-LP as a co-activator of EBNA2 function. J. Gen. Virol. 82:3067–3079.

29. Moore, K. W., R. de Waal Malefyt, R. L. Coffman, and A. O'Garra. 2001. Interleukin-10 and the interleukin-10 receptor. Annu. Rev. Immunol. 19:683–765.

30. Nitsche, F., A. Bell, and A. Rickinson. 1997. Epstein-Barr virus leader protein enhances EBNA-2-mediated transactivation of latent membrane protein 1 expression: a role for the W1W2 repeat domain. J. Virol. 71:6619–6628.

31. Peng, C. W., Y. Xue, B. Zhao, E. Johannsen, E. Kieff, and S. Harada. 2004. Direct interactions between Epstein-Barr virus leader protein LP and the EBNA2 acidic domain underlie coordinate transcriptional regulation. Proc. Natl. Acad. Sci. USA 101:1033–1038.

32. Peng, R., A. V. Gordadze, E. M. Fuentes Panana, F. Wang, J. Zong, G. S. Hayward, J. Tan, and P. D. Ling. 2000. Sequence and functional analysis of EBNA-LP and EBNA2 proteins from nonhuman primate lymphocryptoviruses. J. Virol. 74:379–389.

33. Peng, R., S. C. Moses, J. Tan, E. Kremmer, and P. D. Ling. 2005. The Epstein-Barr virus EBNA-LP protein preferentially coactivates EBNA2-mediated stimulation of latent membrane proteins expressed from the viral divergent promoter. J. Virol. 79:4492–4505.

34. Peng, R., J. Tan, and P. D. Ling. 2000. Conserved regions in the Epstein-Barr virus leader protein define distinct domains required for nuclear localization and transcriptional cooperation with EBNA2. J. Virol. 74:9953–9963.

35. Rabson, M., L. Gradoville, L. Heston, and G. Miller. 1982. Non-immortalizing P3J-HR-1 Epstein-Barr virus: a deletion mutant of its transforming parent, Jijoye. J. Virol. 44:834–844.

36. Radhika, V., D. Onesime, J. H. Ha, and N. Dhanasekaran. 2004. Galpha13 stimulates cell migration through cortactin-interacting protein Hax-1. J. Biol. Chem. 279:49406–49413.

37. Rooney, C., J. G. Howe, S. H. Speck, and G. Miller. 1989. Influence of Burkitt's lymphoma and primary B cells on latent gene expression by the nonimmortalizing P3J-HR-1 strain of Epstein-Barr virus. J. Virol. 63:1531–1539.

38. Rowe, D. T. 1999. Epstein-Barr virus immortalization and latency. Front. Biosci. 4:D346–D371.

39. Sample, J., M. Hummel, D. Braun, M. Birkenbach, and E. Kieff. 1986. Nucleotide sequences of mRNAs encoding Epstein-Barr virus nuclear proteins: a probable transcriptional initiation site. Proc. Natl. Acad. Sci. USA 83:5096–5100.

40. Shaku, F., G. Matsuda, R. Furuya, C. Kamagata, M. Igarashi, M. Tanaka, M. Kanamori, Y. Nishiyama, N. Yamamoto, and Y. Kawaguchi. 2005. Development of a monoclonal antibody against Epstein-Barr virus nuclear antigen leader protein (EBNA-LP) that can detect EBNA-LP expressed in P3HR1 cells. Microbiol. Immunol. 49:477–483.

41. Sharp, T. V., H. W. Wang, A. Koumi, D. Hollyman, Y. Endo, H. Ye, M. Q. Du, and C. Boshoff. 2002. K15 protein of Kaposi's sarcoma-associated herpesvirus is latently expressed and binds to HAX-1, a protein with antiapoptotic function. J. Virol. 76:802–816.

42. Sinclair, A. J., I. Palmero, G. Peters, and P. J. Farrell. 1994. EBNA-2 and EBNA-LP cooperate to cause G_0 to G_1 transition during immortalization of resting human B lymphocytes by Epstein-Barr virus. EMBO J. 13:3321–3328.

43. Speck, S. H., A. Pfitzner, and J. L. Strominger. 1986. An Epstein-Barr virus transcript from a latently infected, growth-transformed B-cell line encodes a highly repetitive polypeptide. Proc. Natl. Acad. Sci. USA 83:9298–9302.

44. Szekely, L., K. Pokrovskaja, W. Q. Jiang, G. Selivanova, M. Lowbeer, N. Ringertz, K. G. Wiman, and G. Klein. 1995. Resting B-cells, EBV-infected B-blasts and established lymphoblastoid cell lines differ in their Rb, p53 and EBNA-5 expression patterns. Oncogene 10:1869–1874.

45. Szekely, L., G. Selivanova, K. P. Magnusson, G. Klein, and K. G. Wiman. 1993. EBNA-5, an Epstein-Barr virus-encoded nuclear antigen, binds to the retinoblastoma and p53 proteins. Proc. Natl. Acad. Sci. USA 90:5455–5459.

46. Taga, S., K. Carlier, Z. Mishal, C. Capoulade, M. Mangeney, Y. Lécluse, D. Coulaud, C. Tétaud, L. L. Pritchard, T. Tursz, and J. Wiels. 1997. Intracellular signalling events in CD77-mediated apoptosis of Burkitt's lymphoma cells. Blood 90:2757–2767.

47. Tang, D., J. M. Lahti, and V. J. Kidd. 2000. Caspase-8 activation and bid cleavage contribute to MCF7 cellular execution in a caspase-3-dependent manner during staurosporine-mediated apoptosis. J. Biol. Chem. 275:9303–9307.

48. Tetaud, C., T. Falguieres, K. Carlier, Y. Lecluse, J. Garibal, D. Coulaud, P. Busson, R. Steffensen, H. Clausen, L. Johannes, and J. Wiels. 2003. Two distinct Gb3/CD77 signaling pathways leading to apoptosis are triggered by anti-Gb3/CD77 MAb and verotoxin-1. J. Biol. Chem. 278:45200–45208.

49. Van Hoof, C., and J. Goris. 2003. Phosphatases in apoptosis: to be or not to be, PP2A is in the heart of the question. Biochim. Biophys. Acta 1640:97–104.

50. Young, L. S., and P. G. Murray. 2003. Epstein-Barr virus and oncogenesis: from latent genes to tumours. Oncogene 22:5108–5121.

51. Young, L. S., and A. B. Rickinson. 2004. Epstein-Barr virus: 40 years on. Nat. Rev. Cancer 4:757–768.